

# Simulation of cross-correlation method for temporal characterization of VUV free-electron-lasers

Wenbin Li (李文斌)\*, Xiaoying Ma (马晓颖), Xiaoyue Yang (杨晓月), and Zhanshan Wang (王占山)

MOE Key Laboratory of Advanced Micro-structure Materials, Institute of Precision Optical Engineering (IPOE),  
School of Physics Science and Engineering, Tongji University, Shanghai 200092, China

\*Corresponding author: wbli@tongji.edu.cn

Received January 29, 2013; accepted June 28, 2013; posted online September 3, 2013

The cross-correlation method for temporal characterization is investigated using simulations of the two-color above threshold ionization (ATI) on He induced by a vacuum ultraviolet (VUV) free-electron laser (FEL) in the presence of an infrared (IR) field. Non-linear dependencies of the sideband structure produced in the two-color ATI process are expressed as a function of IR laser intensity by considering the spatial distributions and temporal jitter of both lasers. The temporal properties of the FEL pulse can be characterized accurately using the cross-correlation method at a low IR laser intensity of  $\sim 3 \times 10^{10}$  W/cm<sup>2</sup> but with low cross-correlation signals. When the dynamic range of sidebands is increased to high IR intensity, the accuracy of the cross-correlation method becomes crucially dependent on the actual non-linear index. An approach of determining this index is proposed here to improve the accuracy of temporal characterizations.

OCIS codes: 140.2600, 020.4180, 320.2250.

doi: 10.3788/COL201311.091403.

Based on the process of self-amplified spontaneous emission (SASE), significant progress has been made on the development of free-electron-lasers (FELs) at the soft and hard X-ray energy regions<sup>[1,2]</sup>. For all experiments employing SASE-FEL, full characterization of these new laser lights, such as determination of their temporal and spectral properties, is important. The pulse duration and arrival time jitter of the laser pulse are vital parameters that must be quantified, especially for time-resolved pump-probe experiments using a two-color scheme<sup>[3-5]</sup>.

An experimental method for measuring the pulse duration and jitter time of SASE-FELs is based on the two-color above threshold ionization (ATI) process on noble gas atoms<sup>[6-8]</sup>. In two-color ATI processes, atomic photoionization is produced by an X-ray photon in the presence of an infrared (IR) laser field. In addition to the single-photon ionization caused by one X-ray photon, free-free transitions can be further induced by the dressing IR laser field, which causes the ionized electron to emit or absorb one or more IR laser photons after the initial ionization. These two-color multiphoton ionization processes result in sideband features on both sides of the main peak in the photoelectron energy spectrum. Since the sideband intensity and structure strongly depend on the IR laser intensity, measurement of the sideband intensity as a function of the time delay via a cross-correlation scheme can be used to characterize the FEL pulse duration and jitter time. Compared with other temporal characterization methods, such as THz streaking<sup>[9,10]</sup> and X-ray induced optical reflectivity change<sup>[11-14]</sup>, this two-color gas phase cross-correlation experiment is a non-destructive diagnostic method that can be used to characterize the pulse duration and jitter time of vacuum ultraviolet (VUV) and X-ray FELs<sup>[8]</sup>. Electro-optical sampling<sup>[15]</sup> is also a non-destructive method but it measures the relative arrival times of electron bunches instead of laser pulses at the experimental interaction region.

According to lowest-order perturbation theory<sup>[16]</sup>, the total population of the  $n$ th sideband is proportional to the intensity of the pump FEL  $I_{\text{FEL}}$  and that of the probe IR laser to the power  $n$ ,  $(I_{\text{IR}})^n$ . If Gaussian profiles are assumed for both laser pulses in the cross-correlation experiment, the full-width at half-maximum (FWHM) of the cross-correlation signals ( $\tau_{\text{C}}$ ) for the  $n$ th sideband is related to the X-ray FEL pulse duration ( $\tau_{\text{FEL}}$ ), the IR laser pulse duration ( $\tau_{\text{IR}}$ ), and the jitter time ( $\tau_{\text{jitter}}$ ) between the FEL and IR laser:

$$\tau_{\text{C}} = \sqrt{\tau_{\text{jitter}}^2 + \tau_{\text{FEL}}^2 + \tau_{\text{IR}}^2} / n. \quad (1)$$

Since free-free transitions are easily saturated, lowest-order perturbation theory rapidly breaks down when the IR laser field becomes more intense<sup>[16]</sup>. Therefore, the simple relationship between the cross-correlation width and the IR pulse duration in Eq. (1) should be corrected as

$$\tau_{\text{C}} = \sqrt{\tau_{\text{jitter}}^2 + \tau_{\text{FEL}}^2 + \tau_{\text{IR}}^2} / \alpha, \quad (2)$$

where the parameter  $\alpha$  represents the effective intensity dependence of the  $n$ th sideband on the IR laser intensity, specifically,  $I_{\text{sb}} \propto (I_{\text{IR}})^\alpha$ . To characterize the FEL pulse duration or jitter time reliably, the parameter  $\alpha$  must be carefully considered. In this letter, the intensity dependencies of the sidebands are studied based on soft-photon approximation (SPA) theory by taking the spatial distributions and temporal jitters of FEL and IR lasers into account. Spatial distributions and temporal jitters strongly influence the intensity of the different orders of sidebands, thereby affecting the accuracy of the temporal characterization based on the cross-correlation method. A novel approach is proposed in this study to determine the actual exponent parameter  $\alpha$  properly and improve accuracy.

SPA theory is an analytical model used to analyze the photoelectron energy spectrum of two-color ATI processes<sup>[17]</sup>. This theoretical model has been proven to agree with more elaborate methods, such as the time-dependent Schrödinger equation, when the photoelectron kinetic energy is considerably larger than the dressing IR laser photon energy<sup>[18]</sup>. In this study, SPA theory was used to simulate the two-color ATI process on atomic He induced by the absorption of an X-ray photon ( $\omega_x$ ) in the IR field ( $\omega_{\text{IR}}$ ). Both laser pulses are assumed to be linearly polarized with parallel polarization in the simulation. According to SPA theory<sup>[17]</sup>, the angle-integrated intensity of the  $n$ th sideband is proportional to the following general form:

$$I_{\text{sb}}^{(n)} \propto \int_0^\pi \sin \theta J_n^2(\alpha_0 k_n \cos \theta) \left( \frac{d\sigma^{(0)}}{d\theta} \right) d\theta, \quad (3)$$

where  $\theta$  denotes the angle between the direction of the polarization of the FEL field and the wave vector of the ejected electron. The parameter  $k_n = \sqrt{2(\omega_x + n\omega_{\text{IR}} - \text{IP} - U_p)}$  is the shifted wave number of the ejected electron with the photoionization threshold of IP and the ponderomotive energy of  $U_p$ ,  $J_n(z)$  is the Bessel function, and  $\alpha_0 = F_{\text{IR}}/\omega^2$  is the classical excursion vector of a free electron embedded in the IR laser field with amplitude  $F_{\text{IR}}$ . The term  $d\sigma^{(0)}/d\theta$  represents the single-photon ionization differential cross-section, which can be expressed as  $1 + \beta(3\cos^2\theta - 1)/2$  with the asymmetry parameter  $\beta = 2$  for the 1-s photoionization of He. Figure 1(a) shows a two-dimensional contour plot of the angle-integrated photoelectron energy spectrum obtained from the two-color ATI of atomic He induced by FEL photons ( $\hbar\omega_x = 90.5$  eV) dressed at different intensities of IR laser fields ( $\hbar\omega_{\text{IR}} \approx 1.55$  eV,  $\lambda_{\text{IR}} = 800$  nm). A FEL photon energy of 90.5 eV is selected because it is a typical photon energy available at the FLASH VUV-FEL facility. As shown in Fig. 1(a), the main He ( $1\text{ s}^{-1}$ ) photoelectron peak at 65.9 eV results from direct photoionization by one FEL photon. On both sides of the main peak, sidebands are situated almost symmetrically and equally separated by an IR photon energy of 1.55 eV. As shown in Fig. 1(b), an increase in IR laser intensity results in increases in the number and intensity of the sidebands and a decrease in the main line. These results are attributed to the fact that the IR laser field does not contribute to the initial ionization process such that the total photoelectron yields for all spectra remain constant. Considering that the sideband intensities are sensitive to the IR laser intensity, the sideband structures can be used to characterize the pulse duration or timing jitter of FELs using Eq. (1). However, Eq. (3) clearly shows that the population of the  $n$ th sideband is proportional to the IR laser intensity raised to the power of  $n$ ,  $(I_{\text{IR}})^n$ , only in the limit of small arguments of the Bessel function, which is consistent with lowest-order perturbation theory. As the IR laser intensity becomes stronger, the simple power law of  $I_{\text{sb}}^{(n)} \propto (I_{\text{IR}})^n$  for the  $n$ th sideband breaks down rapidly, and the sideband intensity may be saturated even at moderate IR laser intensities of  $10^{11}$ – $10^{12}$  W/cm<sup>2</sup>. As shown in Fig. 1, the first-order sideband is already saturated at an IR laser intensity of  $\sim 3.0 \times 10^{11}$  W/cm<sup>2</sup>. Therefore, a complex

non-linear relationship clearly exists between the population of the individual sideband and the IR intensity. To characterize the temporal properties of FEL using the cross-correlation method, the effects of the spatial distribution and temporal jitter on the index of the power law,  $I_{\text{sb}} \propto (I_{\text{IR}})^\alpha$ , must be thoroughly investigated.

To study the effects of the spatially non-uniform intensity distributions of the lasers, the two-color ATI process of He, as shown in Fig. 1, was calculated based on Monte Carlo simulations, where the FEL spot is assumed to have a typical size of  $\sigma_{\text{FEL}} = 50$   $\mu\text{m}$  (FWHM), as used in the FEL facility<sup>[7,8,19]</sup>. The spots of the IR laser may show different FWHM values of  $\sigma_{\text{IR}} = 50, 100,$  and  $150$   $\mu\text{m}$  or be uniformly distributed ( $\sigma_{\text{IR}} \rightarrow \infty$   $\mu\text{m}$ ). The pulse durations for FEL ( $\tau_x$ ) and IR ( $\tau_{\text{IR}}$ ) are assumed to feature typical parameters of 30 and 150 fs, respectively. Synchronization between the FEL and IR laser is considered to be perfect ( $\tau_{\text{jitter}} = 0$  fs) in this case. Figure 2(a) shows the simulated intensities of the first-(SB1), second-(SB2), and third-order (SB3) sidebands as a function of the average IR intensity for different IR spatial distributions. The total intensities of all spectra are normalized

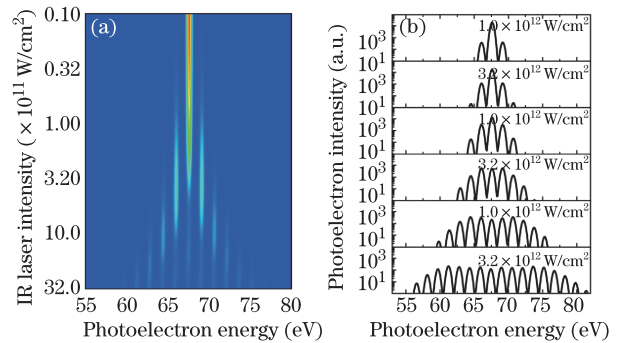


Fig. 1. (Color online) (a) Two-dimensional contour plot of the photoelectron energy spectra obtained from the two-color ATI of He by FEL photons ( $\hbar\omega_x = 90.5$  eV) dressed in an IR laser field ( $\hbar\omega_{\text{IR}} \approx 1.55$  eV) with intensities ranging from  $1.0 \times 10^{10}$  to  $3.2 \times 10^{12}$  W/cm<sup>2</sup>. (b) The corresponding photoelectron energy spectra of (a) in the logarithmic scale at different IR laser intensities.

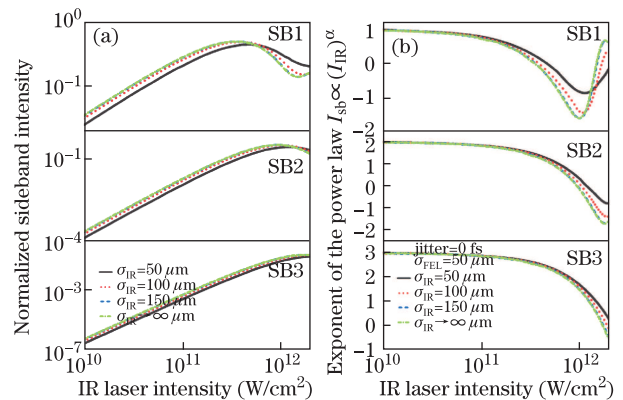


Fig. 2. (Color online) (a) Intensities of the first-order (SB1), the second-order (SB2), and the third-order (SB3) sidebands at spatial distributions of the IR laser with different FWHM ( $\sigma_{\text{IR}}$ ). The jitter time is 0 fs and the FWHM of the Gaussian spatial distribution of FEL is 50  $\mu\text{m}$ . (b) The exponent of the power law  $I_{\text{sb}} \propto (I_{\text{IR}})^\alpha$  for SB1, SB2, and SB3 at spatial and temporal overlap conditions identical to those in (a).

to a constant. Figure 2(a) shows that the sideband intensities of SB1, SB2, and SB3 increase with increasing IR laser spot size under relatively low IR fields of  $1 \times 10^{10} - 3 \times 10^{11} \text{ W/cm}^2$ , likely because ionized electrons generated from larger IR spots experience a stronger effective IR intensity than those generated from smaller IR spots. When the IR laser spot size reaches  $300 \mu\text{m}$ , the sideband yields are nearly identical to those produced from uniformly distributed IR lasers. Thus, if two beams with Gaussian profiles are used in the experiment, the dressing field can be considered homogeneous if the IR beam is at least six times larger than the FEL beam, which is usually the case in the FEL facilities<sup>[8,19]</sup>. Figure 2(a) also shows that low-order sidebands are more easily saturated than high-order sidebands. Additionally, the spatial distribution of the IR laser has a strong effect on the non-linear relationships between the sideband intensities and the IR laser intensity. These non-linear relationships are given in Fig. 2(b) as a function of IR laser intensity by the exponent of the power law  $I_{\text{sb}} \propto (I_{\text{IR}})^\alpha$  for SB1, SB2, and SB3. As predicted by lowest-order perturbation theory, the exponent for the  $n$ th sideband increases asymptotically to the value of  $n$  under weak IR laser intensity ( $1 \times 10^{10} \text{ W/cm}^2$ ). A negative  $\alpha$  value indicates that the sideband intensity is saturated and begins to decrease when the IR laser field becomes stronger. From this simulation, the different spatial distributions of the IR laser are clearly shown to have different effects on the exponent of the power law, especially when the IR laser spot size is less than  $300 \mu\text{m}$ , thereby affecting the cross-correlation results. The dependence of the exponent on the IR spatial distribution is attributed to the fact that the ionized electrons produced inside the FEL spot should be dressed at different IR intensities when the IR laser has a non-uniform distribution. Under a constant average IR intensity, the effective IR intensity is related to the spatial distribution of both lasers, thereby affecting the value of the important parameter  $\alpha$ .

To demonstrate the effects of temporal jitter, the sideband intensities of SB1, SB2, and SB3 are shown in Fig. 3(a) as a function of IR intensity for jitter times of 0, 150, and 300 fs (FWHM). The jitter time between FEL and IR laser is considered to be a Gaussian profile, and the spot sizes of  $\sigma_{\text{FEL}}$  and  $\sigma_{\text{IR}}$  are set to 50 and  $300 \mu\text{m}$ , respectively. As shown in Fig. 3(a), the sideband intensities of SB1, SB2, and SB3 become saturated at stronger laser intensities and longer jitter times because ionized electrons experience a lower effective IR intensity upon inception as the jitter time increases. The intensity dependencies differ among the different orders of sidebands as a function of IR intensity. Exponents of the power law for SB1, SB2, and SB3 are displayed in Fig. 3(b). The exponent varies widely in the vicinity of the saturation intensity region of  $3 \times 10^{11} - 2 \times 10^{12} \text{ W/cm}^2$ . For practical cross-correlation experiments, it is typically performed in the same IR laser intensity region, where low-order sidebands have adequate yield for measurement. However, a strong non-linear relationship exists for low-order sideband intensities in this IR intensity region, as shown in Fig. 3(b). Therefore, temporal characterization based on the cross-correlation method depends critically on the actual exponent parameter  $\alpha$ ,

which is closely related to the temporal jitter and spatial distribution of both lasers.

To demonstrate the intensity dependence of the exponent parameter, cross-correlation signals are simulated for SB1, SB2, and SB3 at three IR laser intensities of  $3 \times 10^{10}$ ,  $3 \times 10^{11}$ , and  $1 \times 10^{12} \text{ W/cm}^2$ , respectively, the results of which are presented in Fig. 4. In this simulation, the jitter time ( $\tau_{\text{jitter}}$ ), pulse duration for FEL ( $\tau_x$ ), and IR ( $\tau_{\text{IR}}$ ) are assumed to be 150, 30, and 150 fs, respectively. The spot sizes of the FEL ( $\sigma_{\text{FEL}}$ ) and IR laser ( $\sigma_{\text{IR}}$ ) are assumed to be 50 and  $300 \mu\text{m}$ , respectively. These parameters are similar to the practical conditions used in the cross-correlation experiments<sup>[7,8,19]</sup>. The cross-correlation signals are fitted using Gaussian profiles to obtain the cross-correlation width  $\tau_C$ , after which the actual exponent  $\alpha$  is estimated using Eq. (2) and given in Fig. 4. Under the cross-correlation signal simulated at an IR intensity of  $3 \times 10^{10} \text{ W/cm}^2$ , the exponents for SB1, SB2, and SB3 are 0.98, 2.03, and 3.06, respectively. These exponents agree well with the perturbative indices predicted by lowest-order perturbation theory, which indicates that

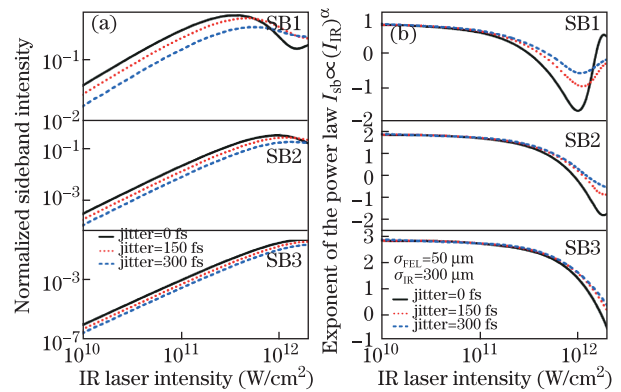


Fig. 3. (Color online) (a) Intensities of the first-order (SB1), the second-order (SB2), and the third-order (SB3) sidebands at different jitter time. The FWHM of the Gaussian spatial distributions of the FEL and IR laser are 50 and  $300 \mu\text{m}$ , respectively. (b) The exponent of the power law  $I_{\text{sb}} \propto (I_{\text{IR}})^\alpha$  for SB1, SB2, and SB3 under spatial and temporal conditions identical to those in (a).

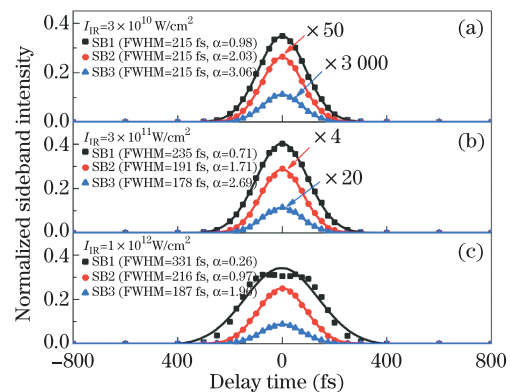


Fig. 4. (Color online) Simulated cross-correlation signals for the first (SB1), the second (SB2), and the third (SB3) sidebands at IR laser intensities of  $3 \times 10^{10}$ ,  $3 \times 10^{11}$ , and  $1 \times 10^{12} \text{ W/cm}^2$ , respectively. Solid lines represent the fitting curves for the corresponding cross-correlation signals.

the cross-correlation method can accurately characterize the temporal properties of FEL pulse at a relatively low IR intensity of  $\sim 3 \times 10^{10}$  W/cm<sup>2</sup>. However, the photoelectron yields of SB2 and SB3 are extremely low at this IR intensity, as shown in Fig. 4(a). Therefore, the accuracy of the cross-correlation method is adequate if only the first sideband is measured with enough statistical parameters. In practical experiments, cross-correlation results are usually measured at relatively high IR intensities ranging from  $10^{11}$  to  $10^{12}$  W/cm<sup>2</sup> for statistical reasons. Figures 4(b) and (c) show the simulated cross-correlation signals obtained at IR intensities of  $3 \times 10^{11}$  and  $1 \times 10^{12}$  W/cm<sup>2</sup>, respectively. From the cross-correlation widths, the exponents for SB1, SB2, and SB3 are estimated to be 0.71, 1.71, and 2.69 at  $I_{\text{IR}} = 3 \times 10^{11}$  W/cm<sup>2</sup>, respectively, and 0.26, 0.97, and 1.96 at  $I_{\text{IR}} = 1 \times 10^{12}$  W/cm<sup>2</sup>, respectively. As the IR laser intensity increases, the exponents become smaller and deviate greatly from the perturbative indices predicted by lowest-order perturbation theory. Therefore, if the perturbative indices are used instead of the actual indices, the pulse duration or the jitter time of FEL pulses cannot be estimated correctly. Knowledge of the actual index of the power law dependence is a prerequisite for characterizing the temporal properties of FEL based on the cross-correlation method.

A direct approach with which to determine the actual index in the cross-correlation experiment is measurement of the dependence of the individual sideband intensity on the IR intensity. However, some difficulties brought about by non-linear effects in the IR saturation region may hinder obtaining reliable exponents. Another approach with which to determine the actual index properly is measurement of the effective IR intensity using the ponderomotive AC Stark shift in the experimental photoelectron energy spectrum, followed by estimation of the actual exponent based on SPA theory according to the effective IR intensity. To validate this approach, the two-color ATI of He shown in Fig. 4(c) was simulated at an average IR intensity of  $10^{12}$  W/cm<sup>2</sup>. The ponderomotive AC Stark shift is estimated to be 36 MeV after considering spatial distributions ( $\sigma_{\text{FEL}} = 50$   $\mu\text{m}$ ,  $\sigma_{\text{IR}} = 300$   $\mu\text{m}$ ) and temporal jitter ( $\tau_{\text{jitter}} = 150$  fs). This energy shift corresponds to an effective IR laser intensity of  $6.0 \times 10^{11}$  W/cm<sup>2</sup>. According to the SPA calculation shown as the green dash-dotted line in Fig. 2(b), the actual indices can be estimated to be 0.81 for SB2 and 2.17 for SB3. Assuming that the FEL and IR laser pulse durations are known, the jitter time can be determined using Eq. (2) to be 134 fs using  $\alpha = 0.81$  for SB2 and 154 fs using  $\alpha = 2.17$  for SB3. While some differences compared with the actual jitter time of 150 fs may be observed, the proposed approach clearly improves the jitter time characterization. Assuming that the jitter time is known, the FEL pulse duration can be estimated to be 44 fs using the cross-correlation signal of SB3 and the parameter  $\alpha$  of 2.17. When the cross-correlation signal of SB2 is used, unacceptable results are obtained for the FEL pulse duration, which demonstrates the drawback of the cross-correlation method for the characterization of very short FEL pulse durations if the exponent parameter cannot be precisely determined. To characterize FEL pulse durations with higher temporal

resolutions, other methodologies are required, such as the auto-correlation method<sup>[20]</sup>. Despite some limitations, the cross-correlation method remains a valid and non-invasive method for online temporal characterizations of X-ray FELs in the hundreds of femtoseconds regime if non-linear effects are considered carefully.

In conclusion, the non-linear dependencies of sideband intensities on the IR intensity during ATI of He induced by FEL photons in the presence of an IR laser are analyzed. Spatial distributions and temporal jitter exert strong effects on the exponent of the power law dependence, which is a crucial parameter required for temporal characterizations of FEL pulses. At low IR intensity ( $\sim 3 \times 10^{10}$  W/cm<sup>2</sup>), the cross-correlation method can be used to characterize the temporal properties of FEL pulses with good precision but poor yield for high-order sidebands. At relatively high IR intensity, determination of the actual non-linear index is proposed. Such an approach can improve the accuracy of temporal characterization. This research provides useful information for determining pulse durations and jitter times based on the cross-correlation method, which is widely adopted in temporal diagnostics of SASE-FEL pulses.

This work was supported by the National Natural Science Foundation of China (No. 11075118) and the Specialized Research Fund for the Doctoral Program of Higher Education (No. 20100072120036).

## References

1. W. Ackermann, G. Asova, V. Ayvazyan, A. Azima, N. Baboi, J. Bähr, V. Balandin, B. Beutner, A. Brandt, A. Bolzmann, R. Brinkmann, O. I. Brovko, M. Castellano, P. Castro, L. Catani, E. Chiadroni, S. Choroba, A. Cianchi, J. T. Costello, D. Cubaynes, J. Dardis, W. Decking, H. Delsim-Hashemi, A. Delsérieys, G. Di Pirro, M. Dohlus, S. Düsterer, A. Eckhardt, H. T. Edwards, B. Faatz, J. Feldhaus, K. Flöttmann, J. Frisch, L. Fröhlich, T. Garvey, U. Gensch, Ch. Gerth, M. Görler, N. Golubeva, H.-J. Grabosch, M. Grecki, O. Grimm, K. Hacker, U. Hahn, J. H. Han, K. Honkavaara, T. Hott, M. Hüning, Y. Ivanisenko, E. Jaeschke, W. Jalmuzna, T. Jezynski, R. Kammering, V. Katalev, K. Kavanagh, E. T. Kennedy, S. Khodyachykh, K. Klöse, V. Kocharyan, M. Körfer, M. Kollé, W. Koprek, S. Korepanov, D. Kostin, M. Krassilnikov, G. Kube, M. Kuhlmann, C. L. S. Lewis, L. Lilje, T. Limberg, D. Lipka, F. Löhler, H. Luna, M. Luong, M. Martins, M. Meyer, P. Michelato, V. Miltchev, W. D. Möller, L. Monaco, W. F. O. Müller, O. Napieralski, O. Napoly, P. Nicolosi, D. Nölle, T. Nuñez, A. Oppelt, C. Pagani, R. Paparella, N. Pchalek, J. Pedregosa-Gutierrez, B. Petersen, B. Petrosyan, G. Petrosyan, L. Petrosyan, J. Pflüger, E. Plönjes, L. Poletto, K. Pozniak, E. Prat, D. Proch, P. Pucyk, P. Radcliffe, H. Redlin, K. Rehlich, M. Richter, M. Roehrs, J. Roensch, R. Romaniuk, M. Ross, J. Rossbach, V. Rybnikov, M. Sachwitz, E. L. Saldin, W. Sandner, H. Schlarb, B. Schmidt, M. Schmitz, P. Schmüser, J. R. Schneider, E. A. Schneidmiller, S. Schnepf, S. Schreiber, M. Seidel, D. Sertore, A. V. Shabunov, C. Simon, S. Simrock, E. Sombrowski, A. A. Sorokin, P. Spanknebel, R. Spesyvtsev, L. Staykov, B. Steffen, F. Stephan, F. Stulle, H. Thom, K. Tiedtke, M. Tischer, S. Toleikis, R. Treusch, D. Trines, I. Tsakov, E. Vogel, T. Weiland, H. Weise, M. Wellhöfer, M. Wendt, I. Will, A. Winter, K. Wittenburg, W. Wurth, P. Yeates, M. V. Yurkov, I. Zagorodnov, and K. Zapfe, *Nature Pho-*

- ton. **1**, 336 (2007).
2. P. Emma, R. Akre, J. Arthur, R. Bionta, C. Bostedt, J. Bozek, A. Brachmann, P. Bucksbaum, R. Coffee, F.-J. Decker, Y. Ding, D. Dowell, S. Edstrom, A. Fisher, J. Frisch, S. Gilevich, J. Hastings, G. Hays, Ph. Hering, Z. Huang, R. Iverson, H. Loos, M. Messerschmidt, A. Miahnahri, S. Moeller, H.-D. Nuhn, G. Pile, D. Ratner, J. Rzepiela, D. Schultz, T. Smith, P. Stefan, H. Tompkins, J. Turner, J. Welch, W. White, J. Wu, G. Yocky, and J. Galayda, *Nature Photon.* **4**, 641 (2010).
  3. J. P. Cryan, J. M. Glowonia, J. Andreasson, A. Belkacem, N. Berrah, C. I. Blaga, C. Bostedt, J. Bozek, C. Buth, L. F. DiMauro, L. Fang, O. Gessner, M. Guehr, J. Hajdu, M. P. Hertlein, M. Hoener, O. Kornilov, J. P. Marangos, A. M. March, B. K. McFarland, H. Merdji, V. S. Petrović, Raman, D. Ray, D. Reis, F. Tarantelli, M. Trigo, J. L. White, W. White, L. Young, P. H. Bucksbaum, and R. N. Coffee, *Phys. Rev. Lett.* **105**, 083004 (2010).
  4. M. Krikunova, T. Maltezopoulos, A. Azima, M. Schlie, U. Frühling, H. Redlin, R. Kalms, S. Cunovic, N. M. Kabachnik, M. Wieland, and M. Drescher, *New J. Phys.* **11**, 123019 (2009).
  5. Q. Zhou and X. Zhang, *Chin. Opt. Lett.* **9**, 110006 (2011).
  6. T. E. Glover, R. W. Schoenlein, A. H. Chin, and C. V. Shank, *Phys. Rev. Lett.* **76**, 2468 (1996).
  7. M. Meyer, D. Cubaynes, P. O’Keeffe, H. Luna, P. Yeates, E. T. Kennedy, J. T. Costello, P. Orr, R. Taïeb, A. Maquet, S. Düsterer, P. Radcliffe, H. Redlin, A. Azima, E. Plönjes, and J. Feldhaus, *Phys. Rev. A* **74**, 011401 (2006).
  8. S. Düsterer, P. Radcliffe, C. Bostedt, J. Bozek, A. L. Cavalieri, R. Coffee, J. T. Costello, D. Cubaynes, L. F. DiMauro, Y. Ding, G. Doumy, F. Grüner, W. Helml, W. Schweinberger, R. Kienberger, A. R. Maier, M. Messerschmidt, V. Richardson, C. Roedig, T. Tschentscher, and M. Meyer, *New J. Phys.* **13**, 093024 (2011).
  9. U. Frühling, M. Wieland, M. Gensch, T. Gebert, B. Schütte, M. Krikunova, R. Kalms, F. Budzyn, O. Grimm, J. Rossbach, E. Plönjes, and M. Drescher, *Nature Photon.* **3**, 523 (2009).
  10. I. Grguraš, A. R. Maier, C. Behrens, T. Mazza, T. J. Kelly, P. Radcliffe, S. Düsterer, A. K. Kazansky, N. M. Kabachnik, T. Tschentscher, J. T. Costello, M. Meyer, M. C. Hoffmann, H. Schlarb, and A. L. Cavalieri, *Nature Photon.* **6**, 851 (2012).
  11. C. Gahl, A. Azima, M. Beye, M. Deppe, K. Döbrich, U. Hasslinger, F. Hennies, A. Melnikov, M. Nagasono, A. Pietzsch, M. Wolf, W. Wurth, and A. Föhlisch, *Nature Photon.* **2**, 165 (2008).
  12. M. R. Bionta, H. T. Lemke, J. P. Cryan, J. M. Glowonia, C. Bostedt, M. Cammarata, J. C. Castagna, Y. Ding, D. M. Fritz, A. R. Fry, J. Krzywinski, M. Messerschmidt, S. Schorb, M. L. Swiggers, and R. N. Coffee, *Opt. Express* **19**, 21855 (2011).
  13. S. Schorb, T. Gorkhover, J. P. Cryan, J. M. Glowonia, M. R. Bionta, R. N. Coffee, B. Erk, R. Boll, C. Schmidt, D. Rolles, A. Rudenko, A. Rouzee, M. Swiggers, S. Carron, J. C. Castagna, J. D. Bozek, M. Messerschmidt, W. F. Schlotter, and C. Bostedt, *Appl. Phys. Lett.* **100**, 121107 (2012).
  14. M. Beye, O. Krupin, G. Hays, A. H. Reid, D. Rupp, S. de Jong, S. Lee, W. S. Lee, Y. D. Chuang, R. Coffee, J. P. Cryan, J. M. Glowonia, A. Föhlisch, M. R. Holmes, A. R. Fry, W. E. White, C. Bostedt, A. O. Scherz, H. A. Durr, and W. F. Schlotter, *Appl. Phys. Lett.* **100**, 121108 (2012).
  15. A. Azima, S. Düsterer, P. Radcliffe, H. Redlin, N. Stojanovic, W. Li, H. Schlarb, J. Feldhaus, D. Cubaynes, M. Meyer, J. Dardis, P. Hayden, P. Hough, V. Richardson, E. T. Kennedy, and J. T. Costello, *Appl. Phys. Lett.* **94**, 144102 (2009).
  16. A. Bouhal, R. Evans, G. Grillon, A. Mysyrowica, P. Breger, P. Agostini, R. C. Constantinescu, H. G. Muller, and D. von der Linde, *J. Opt. Soc. Am. B* **14**, 950 (1997).
  17. A. Maquet and R. Taïeb, *J. Mod. Opt.* **54**, 1847 (2007).
  18. M. Meyer, D. Cubaynes, D. Glijer, J. Dardis, P. Hayden, P. Hough, V. Richardson, E. T. Kennedy, J. T. Costello, P. Radcliffe, S. Düsterer, A. Azima, W. B. Li, H. Redlin, J. Feldhaus, R. Taïeb, A. Maquet, A. N. Grum-Grzhimailo, E. V. Gryzlova, and S. I. Strakhova, *Phys. Rev. Lett.* **101**, 193002 (2008).
  19. P. Radcliffe, M. Arbeiter, W. B. Li, S. Düsterer, H. Redlin, P. Hayden, P. Hough, V. Richardson, J. T. Costello, T. Fennel, and M. Meyer, *New J. Phys.* **14**, 043008 (2012).
  20. R. Moshhammer, Th. Pfeifer, A. Rudenko, Y. H. Jiang, L. Foucar, M. Kurka, K. U. Kühnel, C. D. Schröter, J. Ullrich, O. Herrwerth, M. F. Kling, X. J. Liu, K. Motomura, H. Fukuzawa, A. Yamada, K. Ueda, K. L. Ishikawa, K. Nagaya, H. Iwayama, A. Sugishima, Y. Mizoguchi, S. Yase, M. Yao, N. Saito, A. Belkacem, M. Nagasono, A. Higashiya, M. Yabashi, T. Ishikawa, H. Ohashi, H. Kimura, and T. Togashi, *Opt. Express* **19**, 21698 (2011).